ALCHEMY Jurnal Penelitian Kimia

Official Website: https://jurnal.uns.ac.id/alchemy

ISSN 1412-4092
EISSN 2443-4183

Preparation and Characterization of Carbon/Si Nanocomposites Synthesized by Chemical Vapor Deposition (CVD) Using SiC and SiO_2

Retno Duwi Hardini[a], Teguh Endah Saraswati[a*], Sentot Budi Rahardjo[a], Alaa Keshtta[b]

[a]*Department of Chemistry, Faculty of Mathematics and Natural Sciences, Sebelas Maret University*
Jalan Ir. Sutami 36 A, Kentingan, Surakarta, 57126, Indonesia
[b]*Department of Production Engineering and Mechanical Design, Faculty of Engineering, Port Said University*
Port Said, 42526, Egypt

[*]*Corresponding author: teguh@mipa.uns.ac.id*

DOI: 10.20961/alchemy.20.2.80438.218-225

Received 15 November 2023, Revised 8 December 2023, Accepted 11 September 2024, Published 30 September 2024

Keywords:

carbon nanocomposites;
CVD;
SiC;
SiO_2.

ABSTRACT. Carbon-based nanocomposite materials have attracted the attention of researchers in the last decade due to their unique properties applicable in wide applications. This study aims to synthesize and study the characteristics of the carbon-based nanocomposite material produced using the chemical vapor deposition (CVD) method with SiC and SiO_2. The CVD process was carried out at 900 °C in a vacuum with flowing argon, hydrogen, and acetylene gases. The CVD process produced nanocomposites with more sp^3 hybridized carbon atoms, as indicated by the D peak in the Raman spectra. The diffraction pattern analyses show that the resulting carbon powder nanocomposite growth with SiC powder (CSiC) reveals a carbon diffraction peak C(002) and has an elongated form confirmed by an electron microscope. In comparison, the resulting carbon powder nanocomposite growth with SiO_2 powder (C_{SiO2}) has a spherical form and presents a carbon diffraction peak C(002). C_{SiC} nanocomposites showed both symmetric and asymmetric C–H stretching. In FTIR data, C_{SiO2} nanocomposites show more intense O–H group peaks but lower-intensity C–H group vibrations.

INTRODUCTION

Carbon is an element that is easily obtained and abundant in nature. Carbon materials, one of the most abundant materials on earth, can be found in nature, such as graphite, diamonds, and coal (Maduraiveeran and Jin, 2021). Carbon is found in several different hybridization states, each with unique properties. Carbon allotropes' electrical, thermal, mechanical, and chemical properties are directly correlated with their hybridization state and structure. Carbon allotropes in nanometers, i.e., called carbon nanomaterials, have various sizes and dimensions. Carbon generally has allotropes, which can be classified based on their dimensional structure. Carbon allotropes with zero dimensions (0D) include carbon dots, carbon onions, fullerenes, and nanodiamonds; one-dimensional (1D) carbon allotropes include carbon nanofibers, carbon nanohorns, and carbon nanotubes (CNT); two-dimensional (2D) carbon allotropes include graphene; and three-dimensional (3D) carbon allotrope include multi-layered graphitic nanosheets and diamond (Giraud *et al.*, 2021). Carbon materials can be referred to as carbon nanomaterials when the diameter size of the particle or fiber ranges from about 1 nm to 100 nm. Carbon nanomaterials, with their excellent properties, are ideal candidates for advanced applications in the fields of electronics, membranes, wastewater treatment, batteries, capacitors, heterogeneous catalysis, as well as biological and medical sciences (Manawi *et al.*, 2018; Cai *et al.*, 2019).

Various techniques have been reported in the literature for synthesizing 0D, 1D, 2D, and 3D carbon nanomaterials. The most common techniques for preparing carbon nanomaterials are laser ablation (Wang *et al.*, 2022), arc discharge (Zhang *et al.*, 2019), and chemical vapor deposition (CVD) (He *et al.*, 2009; Manawi *et al.*, 2018; Saraswati *et al.*, 2020b). CVD is the most common technique to prepare thin film deposition technique. This technology mainly uses one or more compounds or gas phase elements containing target product elements to carry out chemical reactions on the substrate surface to produce products (Saputri *et al.*, 2020; Garg *et al.*, 2024; Ivanov

Cite this as: Hardini, R. D., Saraswati, T. E., Rahardjo, S. B., and Keshtta, A., 2024. Preparation and Characterization of Carbon/Si Nanocomposites Synthesized Using Chemical Vapor Deposition (CVD) Using SiC and SiO_2. *ALCHEMY Jurnal Penelitian Kimia*, 20(2), 218-225. https://dx.doi.org/10.20961/alchemy.20.2.80438.218-225.

Copyright © 2024, Universitas Sebelas Maret, ISSN 1412-4092, e ISSN 2443-4183

et al., 2024; Nánai *et al*., 2024). CVD has been widely used to develop crystals and deposit various single crystals, polycrystallines, or inorganic thin films such as glass (Lee *et al*., 2021). Moreover, as a valuable research industry and industrial production method, CVD technology has become one of the most classic methods for preparing various carbon nanomaterials (Saraswati *et al*., 2017; Saraswati *et al*., 2020a; Prasiwi *et al*., 2021; Priyanti *and* Saraswati, 2021; Muchlisha *et al*., 2023). In this process, gas components react on the surface of the wafer and form a thin layer. The economically friendly and easy experimental setup is one of the reasons for choosing CVD as a method to synthesize carbon nanomaterials. Many hydrocarbons can be used as precursors in various compound states, namely gas, liquid, or solid. The energy used for the breakdown and excitation of molecules includes heat, plasma, radiation, metal-organic high energy species via thermal CVD, plasma-enhanced CVD (PECVD), radiation-enhanced CVD, and metal-organic vapor deposition (MOCVD), respectively. The reactions that occur in the CVD method are thermal decomposition reactions, reduction reactions, disproportionation reactions, and couple reactions (Cahay *et al*., 2014).

CVD can also be used as a technique to modify the surface properties of components by engineering layers of components with layers of other metals or other compounds through chemical reactions in the vapor phase at high temperatures. CVD is widely applied in material manufacturing technology. The majority of these applications involve coating or coating solids on the surface. Another application of CVD is to produce high-purity bulk material and powder (Brindhadevi *et al*., 2023). The CVD technique is used to manufacture thin films, which are used in the microelectronics industry as dielectrics, conductors, passivation layers, oxidation barriers, and epitaxy layers. Fiber optic production is resistant to corrosion and heat resistant. The other applications of the CVD technique are for manufacturing high-temperature materials, such as tungsten and ceramics, manufacturing materials used in solar cells, manufacturing superconductor materials, and manufacturing high-temperature-resistant carbon nanocomposites (Anggoro *et al*., 2022).

Carbon nanocomposites have received much attention in various fields due to their extraordinary properties (Speranza, 2021; Javed *et al*., 2024; Lei *et al*., 2024; Luo *et al*., 2024). The desired elements in carbon nanocomposites can be designed by choosing the appropriate powder substrate used in CVD as a place for carbon growth, e.g., ceramic (Jagani *et al*., 2024), silicates (zeolite, montmorillonite, kaolinite) (Kadlečíková *et al*., 2024), Al_2O_3, MgO (Mohana *et al*., 2024), resulting in carbon nanocomposite materials. The common powder substrate material selected in CVD generally has a high surface area and provides catalytic activity supporting the chemical reaction during the CVD process. However. to the best of the authors' knowledge, the growth of carbon nanocomposites using SiO_2 and SiC has not been widely explored in CVD, nor has the characterization of their products. Therefore, this study reports the synthesis of carbon/silica nanocomposite using the CVD method and their characterization. The results reported might give necessary information to other researchers that will benefit the development of carbon-based nanomaterials.

MATERIALS AND METHODS

The materials used are SiC powder (technical grade), SiO_2 powder (technical grade), distilled water, ethanol (99%, Merck), argon gas, acetylene gas, and hydrogen gas (PT. Samator gas industry, UHP grade). Instruments used are X-ray diffractometer (XRD) (Bruker D8 Advance; Cu 1.54 nm; 40 V), scanning electron microscope (SEM) with energy dispersive x-ray spectroscopy (EDX) (Hitachi SU 3500 brand), Fourier-transform infrared (FTIR) (Shimadzu IR Prestige-21), and Raman spectroscopy (Modular Raman Type iHR 320; laser 532 nm).

Synthesis of carbon nanocomposites using the CVD method

This CVD method was carried out using acetylene, hydrogen, and argon gas sources in a flow gas ratio (L/min) of 1:2:1. The powder substrate used was SiO_2 powder and SiC powder put in a separate alumina boat and placed in an OTF quarts furnace with a balanced position. The CVD equipment consisted of a quartz tube with a horizontal furnace connected to the gas inlet and outlet hoses. The inlet gas hose was connected to the gas source, and the outlet gas hose was attached to the vacuum pump. Argon gas was supplied when the furnace temperature reached 350 °C to remove the remaining water vapor in the furnace. The other gases flowed to the chamber at a temperature-increasing rate of 200 °C/40 min. The temperature chamber was set to 900 °C for 10 min. The resulting material is labeled C_{SiC} nanocomposite and C_{SiO2} nanocomposite.

The synthesized nanocomposites were characterized using XRD. The surface morphology of the nanocomposite solids was analyzed using SEM-EDX. The data obtained by imaging mode from the SEM test

Copyright © 2024, Universitas Sebelas Maret, ISSN 1412-4092, e ISSN 2443-4183

results in images of the nanoparticle surface at a certain magnification resolution. The constituent elements of the nanoparticles formed were analyzed using energy-dispersive X-ray spectroscopy (EDX) to determine the constituent elements. The data obtained are elemental mapping and peak intensity data, which show the percentage (%) of the elements that comprise the synthesized nanoparticles. Other instruments used for analysis are FTIR and Raman spectroscopy to the molecular vibrational spectra.

RESULTS AND DISCUSSION

Carbon nanocomposites/Si compounds have been successfully synthesized using the CVD method with two powder substrates, SiO_2 and SiC. This CVD process was carried out in a closed system with gas flow, and the CVD equipment circuit is shown in Figure 1.

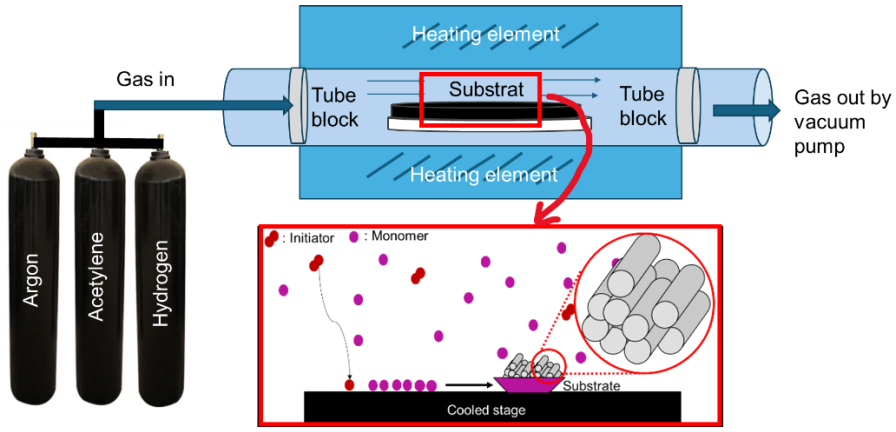

Figure 1. CVD experimental setup.

Synthesis of carbon nanocomposites/Si compounds using the CVD method resulted in growth in quarts boats containing white SiO_2 powder and SiC in the form of greenish powder (see Figure 2(a)), which turned into black powder as in Figure 2(b). In the CVD process, all atmospheric gases in the chamber are initially removed to avoid oxidation processes caused by oxygen-containing gases in the atmosphere. Carbon precursor gas (especially hydrocarbons) flows into the reaction chamber with inert gases such as helium or argon. When the furnace was turned on, the gases evaporated and decomposed, resulting in a reaction between the reactive species derived from the gas and the catalyst, yielding carbon deposition on the powder substrate. Gas decomposition occurs in the temperature range of 600 – 1200 °C. The hydrocarbon decomposed to be species, i.e., hydrogen and carbon, further interacts with the metal catalyst. Carbon will dissolve into the metal, while hydrogen gas will be evaporated out, leaving the chamber pumped out by the vacuum pump.

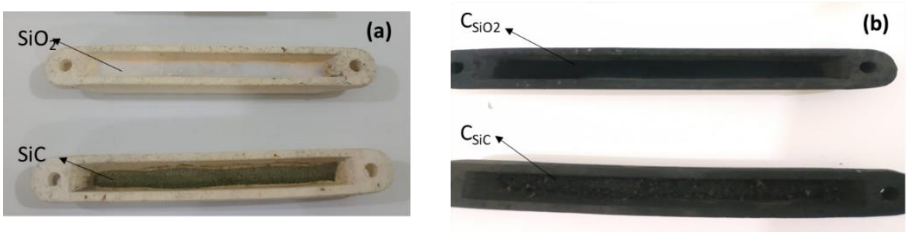

Figure 2. SiC and SiO_2 powder substrates in alumina boat (a) before the CVD process and (b) after the CVD process.

The XRD peak identification is carried out by comparing the 2θ values of the synthesized diffractogram peaks to the 2θ values of the Joint Committee on Powder Diffraction Standard (JCPDS) reference data. The diffractogram results of C_{SiC} nanocomposites and C_{SiO2} nanocomposites resulting from CVD synthesis can be seen in Figure 3 (A and B). Figure 3(A) shows the XRD spectrum of the C_{SiC} nanocomposite presenting a carbon peak C (002) at 2θ 26.603° in accordance with JCPDS standard number Carbon 26-1076. Carbon peaks also appear at 2θ 42.717°, 43.450°, and 46.308° in accordance with the carbon diffraction database in JCPDS 26-1076 as peaks of C (101), (102), (104), respectively. Apart from the carbon peak, the C_{SiC} nanocomposite diffraction spectrum also reveals a Si peak at 2θ 30.102° as SiO_2 (110) in accordance with JCPDS number 88-2486. The SiO_2 peak was

Copyright © 2024, Universitas Sebelas Maret, ISSN 1412-4092, e ISSN 2443-4183

also identified at 2θ 39.957°, 43.091°, 45.609°, and 60.181° as peaks of SiO_2 (101), (200), (111), and (211). Figure 3(A) shows that Si compound carbon nanocomposites can be formed in the CVD process with a SiC powder substrate, indicated by the presence of carbon peaks and Si compounds in the XRD spectra after synthesis. Si compound carbon nanocomposites were also formed with SiO_2 powder substrate. The XRD spectra of C_{SiO2} nanocomposites are shown in Figure 3(B). The C_{SiO2} nanocomposite shows a carbon peak at 2θ 26.228° C (002) and a peak at 2θ 44.363° C (101).

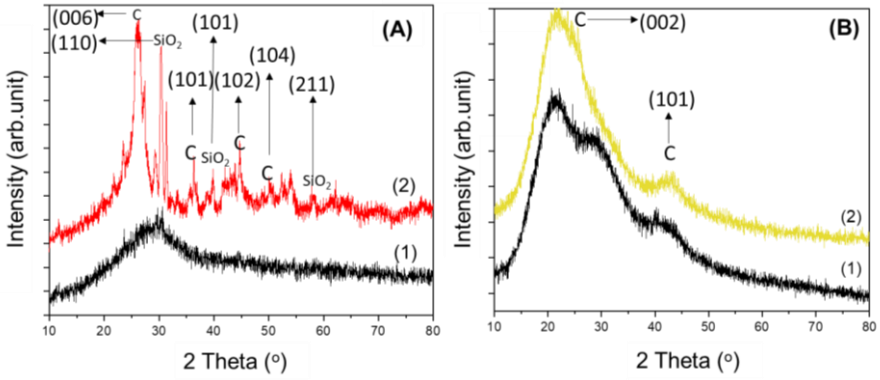

Figure 3. XRD spectra of SiC (A1); C_{SiC} nanocomposite (A2); SiO_2 subsrate (B1); and C_{SiO2} nanocomposite (B2).

C_{SiC} nanocomposites and C_{SiO2} nanocomposites were further analyzed using a scanning electron microscope (SEM) with energy-dispersive X-ray spectroscopy (EDX) to support XRD analysis data and determine surface morphology and element content. SEM analysis is equipped with the EDX feature to determine the composition of the constituent elements of the nanocomposites resulting from the CVD method. The results of the SEM analysis are images shown in Figure 4. The morphology of the initial SiC powder substrate structure is in the form of large irregular chunks, as observed on the material's surface, as shown in Figure 4(a). However, after the CVD process, the resulting C_{SiC} nanocomposite produces a different surface morphology resembling an irregular with various sizes overlapping each other, as shown in Figure 4(b). Meanwhile, the C_{SiO2} nanocomposite shows no significant differences. Figure 4(c and d) shows that the observed morphology shows a spherical form as the initial SiO_2 powder substrate. However, the C_{SiO2} nanocomposite has additional carbon element content, as analyzed in the following EDX spectra data.

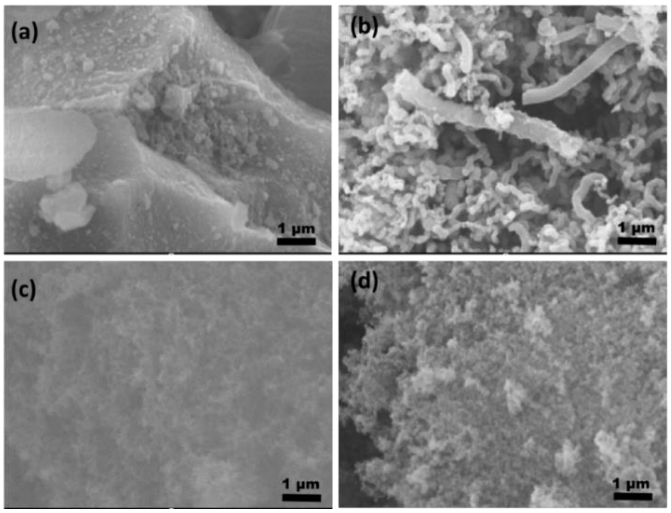

Figure 4. SEM images of (a) SiC; (b) C_{SiC} nanocomposite; (c) SiO_2; (d) C_{SiO2} nanocomposite.

The EDX spectra, as presented in Figure 5, show that the elemental analysis of CVD carbon products using SiC powder significantly reveals different compositions before and after the synthesis process. Before the CVD process, the initial SiC powder contained 74.75% element C and 25.25% element Si. However, after the CVD process, the carbon product has the dominant C element of almost 100%. In contrast, the Si element was not significantly detected, possibly due to the shallow content of Si. Similarly, the CVD carbon product using SiO_2

Copyright © 2024, Universitas Sebelas Maret, ISSN 1412-4092, e ISSN 2443-4183

initially did not contain a C element; however, after the synthesis process, the C element was detected as 32.86%, indicating that the carbon growth successfully occurred during CVD process.

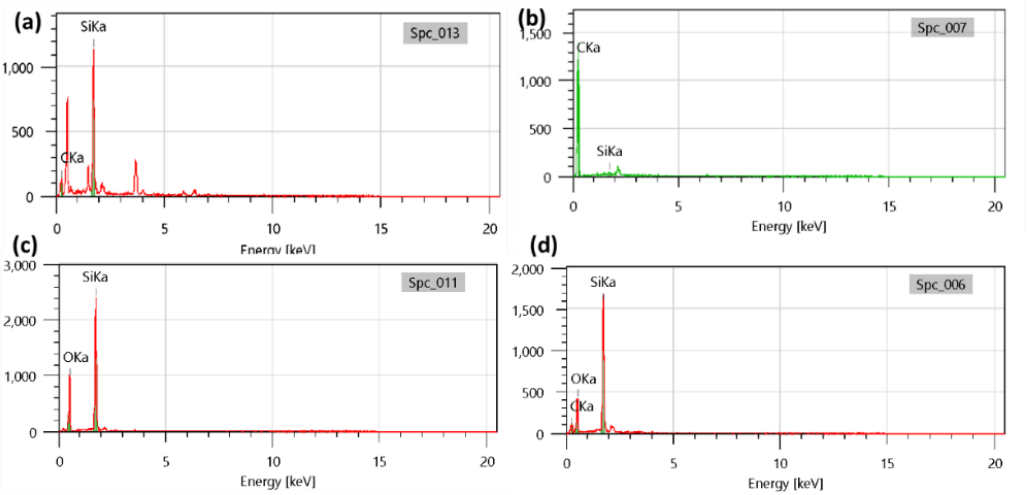

Figure 5. EDX spectra of (a) SiC, (b) C_{SiC} nanocomposite, (c) SiO_2, and (d) C_{SiO2} nanocomposite.

Figure 6 (a and b) shows the FTIR profiles of SiC and SiO_2 before and after the CVD process. Both figures show that a broadband absorption at a wavenumber of ~3440 cm^{-1} in the C_{SiC} nanocomposite (Figure 6a) represents an O–H vibration. This group vibration intensity increased significantly after the CVD process, as observable in the FTIR profile of the C_{SiC} nanocomposite. In addition, the strong band at wavenumber ~1100 cm^{-1} represents the absorption of the Si–O–Si group, which is significantly observable in the initial SiO_2 powder substrate and was indeed not present in the initial SiC powder substrate. However, after the CVD process, the peak intensity of the Si–O–Si group significantly decreased in C_{SiO2} and increased in C_{SiC} nanocomposite. Moreover, the carbon nanocomposite/Si compound shows several other group absorptions, including symmetric and asymmetric stretching of C–H (~2900 cm^{-1}) and (~2800 cm^{-1}).

Compared to the resulting C_{SiC} nanocomposite, the C_{SiO2} nanocomposite has slightly shifted wavenumber for O–H and O–H groups. The broad O–H absorption band is observed at ~3453 cm^{-1} for C_{SiO2} nanocomposite while at 3447.3 cm-1 for C_{SiC}. Besides being observable at ~800 cm^{-1}, the wide band for Si–O–Si is also observable at ~1111 cm^{-1} for C_{SiO2} and 1019 cm^{-1} for C_{SiC} nanocomposite. Moreover, besides having O–H and Si–O–Si group absorption, the C_{SiO2} nanocomposite also has C–H group absorption with low intensity at ~2923 cm^{-1} and ~2856 cm^{-1}, which are close to those peaks in C_{SiC} nanocomposite.

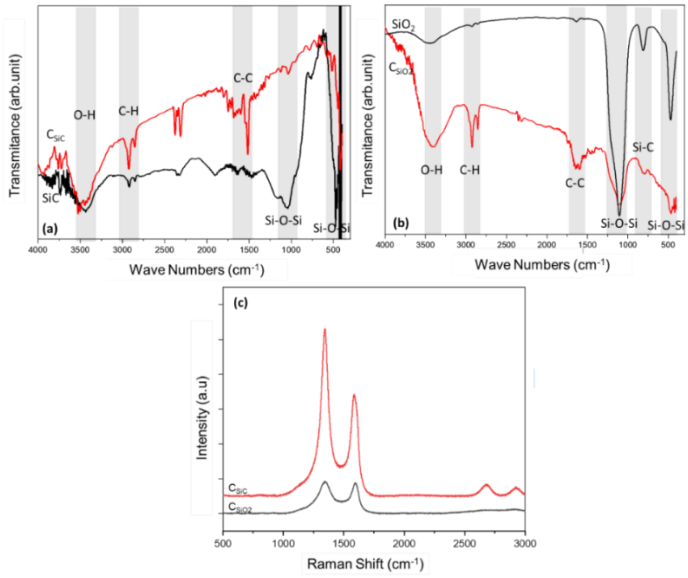

Gambar 6. FTIR spectra of (a) SiC and C_{SiC} nanocomposite, (b) SiO_2 and C_{SiO2} nanocomposite; (c) Raman spectra of C_{SiC} nanocomposites and C_{SiO2} nanocomposites.

Copyright © 2024, Universitas Sebelas Maret, ISSN 1412-4092, e ISSN 2443-4183

The Raman spectra of C_{SiC} nanocomposites and C_{SiO2} nanocomposites are shown in Figure 6(c) and Table 1. C_{SiC} nanocomposites in Figure 6(c) show peak D at a Raman shift of 1347.21 cm^{-1}, G band at a Raman shift of 1587.60 $cm^{-1,}$ and G' band at a Raman shift of ~2700 cm^{-1}. The C_{SiO2} nanocomposite in Figure 6(c) shows peak D at Raman shift 1343.01 cm^{-1} and G band at 1595.24 cm^{-1}. Both Raman spectra of nanocomposites C_{SiO2} and C_{SiC} reveal a higher D band intensity than the G band intensity. This phenomenon indicates that the synthesized product has dominant sp^3 bonds compared to sp^2 bonds. The Raman intensity in Figure 6(c) and Table 1 shows that the C_{SiC} nanocomposite has a higher intensity compared to the C_{SiO2} nanocomposite; this indicates that the C_{SiC} nanocomposite has the highest graphite. The irregularity in the material is shown by the results of the highest I_D/I_G value being the C_{SiC} nanocomposite, followed by the C_{SiO2} I_D/I_G value nanocomposite, as shown in Table 1. The higher the I_D/I_G value, the higher the defect structure formed. The appearance of the G' band indicates structural modifications that represent the existence of other structures of carbon allotropes. The presence of the D band, G band, and G' band in the carbon/Si compound nanocomposite with SiC powder substrate indicates the presence of metals such as Si in the nanocomposite; this is confirmed according to the XRD results. The carbon nanocomposite/Si compound with SiO_2 powder substrate does not show any G' band peak, which indicates that there are no compounds other than carbon allotropes so that the D band and G band have almost the same optimal intensity.

Table 1. Intensity of D band (I_D), G band (I_G), G' band ($I_{G'}$), and I_D/I ratio.

Nanocomposites	I_D	I_G	$I_{G'}$	I_D/I_G
C_{SiC}	1347.21	1587.60	2691.61	0.848
C_{SiO2}	1342.01	1595.24	-	0.841

CONCLUSION

The CVD process produces more carbon nanocomposites, producing a sp^3 carbon structure, as shown by the Raman shift results. The results of the diffraction pattern analysis show that the synthesis results with the SiC powder substrate show a carbon diffraction peak C (006), and the synthesis results with the SiO_2 powder substrate show a carbon diffraction peak C (002). Carbon nanocomposites with SiC powder substrates show symmetric and asymmetric C–H stretching. Carbon nanocomposites with SiO_2 powder substrates absorb O–H groups. Apart from that, it also has low-intensity C–H group absorption. The results of the morphological analysis of the Si compound nanocomposites show that the carbon nanocomposites with SiC powder substrates are elongated fibers, and the carbon nanocomposites with SiO_2 powder substrates are round.

CONFLICT OF INTEREST

There is no conflict of interest in this article.

AUTHOR CONTRIBUTION

RDH: Data Analysis, Initial Manuscript Drafting; TES: Conceptualization, Methodology, Data Validation, Manuscript Review and Editing, Supervision; SBR: Conceptualization, Supervision; AK: Manuscript Revision.

ACKNOWLEDGMENT

This research was supported by the Research Fund program of the Ministry of Education, Culture, Research and Technology of the Republic of Indonesia for providing the research grant No. 1280.1/UN27.22/PT.01.03/2023.

REFERENCES

Anggoro, P. A., Saraswati, T. E. and Raharjo, W. W., 2022. Synthesis of Magnetic Carbon Nanotubes (Mag-Cnt) by Chemical Vapor Deposition (CVD) Method and Modification for CNT/Epoxy Resin Composite Filler. *Journal of Physics: Conference Series* 2190 (1). https://doi.org/10.1088/1742-6596/2190/1/012024.

Brindhadevi, K., Garalleh, H. A. L., Alalawi, A., Al-Sarayreh, E. and Pugazhendhi, A., 2023. Carbon Nanomaterials: Types, Synthesis Strategies and Their Application as Drug Delivery System for Cancer Therapy. *Biochemical Engineering Journal* 192. https://doi.org/10.1016/j.bej.2023.108828.

Copyright © 2024, Universitas Sebelas Maret, ISSN 1412-4092, e ISSN 2443-4183

Cahay, M., Murray, P. T., Back, T. C., Fairchild, S., Boeckl, J., Bulmer, J., Koziol, K. K. K., Gruen, G., Sparkes, M., Orozco, F. and O'neill, W., 2014. Hysteresis During Field Emission from Chemical Vapor Deposition Synthesized Carbon Nanotube Fibers. *Applied Physics Letters* 105 (17). https://doi.org/10.1063/1.4900787.

Cai, W., Chen, C. H., Chen, N. and Echegoyen, L., 2019. Fullerenes as Nanocontainers That Stabilize Unique Actinide Species Inside: Structures, Formation, and Reactivity. *Accounts of Chemical Research* 52 (7), 1824-1833. https://doi.org/10.1021/acs.accounts.9b00229.

Garg, R., Ghosh, A. and Arya, A. K., 2024. Synthesis of Nano-Silicon Carbide by SiO–C Reaction. *Ceramics International* 50 (20, Part B), 39080-39087. https://doi.org/10.1016/j.ceramint.2024.07.274.

Giraud, L., Tourrette, A. and Flahaut, E., 2021. Carbon Nanomaterials-Based Polymer-Matrix Nanocomposites for Antimicrobial Applications: A Review. *Carbon* 182, 463-483. https://doi.org/10.1016/j.carbon.2021.06.002.

He, C. N., Zhao, N. Q., Shi, C. S. and Song, S. Z., 2009. Fabrication of Carbon Nanomaterials by Chemical Vapor Deposition. *Journal of Alloys and Compounds* 484 (1), 6-11. https://doi.org/10.1016/j.jallcom.2009.04.088.

Ivanov, I., Marinov, S., Popov, G., Abrashev, M., Kirilov, K. and Kiss'ovski, Z., 2024. Deposition of Carbon Nanolayers by Pecvd on Ceramic Substrates. *Journal of Physics: Conference Series* 2710 (1), 012006. https://doi.org/10.1088/1742-6596/2710/1/012006.

Jagani, S. A., Dai, J., Acauan, L., and Wardle, B. L., 2024. Fabrication and Processing of Aligned Boron Nitride and Carbon Nanotubes for Nanocomposite Systems. *AIAA Scitech 2024 Forum*. https://doi.org/10.2514/6.2024-1005.

Javed, A., Islam, M., Al-Ghamdi, Y. O., Iqbal, M., Aljohani, M., Sohni, S., Shah, S. S. A. and Khan, S. A., 2024. Synthesis of Oxidized Carboxymethyl Cellulose-Chitosan and Its Composite Films with SiC and SiC@SiO_2 Nanoparticles for Methylene Blue Dye Adsorption. *International Journal of Biological Macromolecules* 256, 128363. https://doi.org/10.1016/j.ijbiomac.2023.128363.

Kadlečíková, M., Škriniarová, J., Breza, J., Jesenák, K. and Bédiová, K., 2024. Silicate Substrates Used to Anchor Iron Particles Catalysing the Formation of Carbon Nanotubes. *AIP Conference Proceedings* 3054 (1). https://doi.org/10.1063/5.0187460.

Lee, S.-H., Park, J., Park, J. H., Lee, D.-M., Lee, A., Moon, S. Y., Lee, S. Y., Jeong, H. S. and Kim, S. M., 2021. Deep-Injection Floating-Catalyst Chemical Vapor Deposition to Continuously Synthesize Carbon Nanotubes with High Aspect Ratio and High Crystallinity. *Carbon* 173, 901-909. https://doi.org/10.1016/j.carbon.2020.11.065.

Lei, D., Liu, C., Wang, S., Liu, J., Zhang, P., Li, Y., Yin, B., Bao, J., Dong, C., Liu, Z. and Su, Y., 2024. Ultrabroad Electromagnetic Absorbing Core-Shell SiC@SiO_2 Nanocomposites Derived from in Situ Oxidation SiC Whiskers. *Journal of Alloys and Compounds* 994, 174637. doi: https://doi.org/10.1016/j.jallcom.2024.174637.

Luo, Y., He, Q., Wang, Y. and Yin, X., 2024. Preparation and Electromagnetic Waves Absorption Performance of Novel Fe_3Si/SiC/SiO_2 Composites. *Journal of Alloys and Compounds* 1003, 175617. doi: https://doi.org/10.1016/j.jallcom.2024.175617.

Maduraiveeran, G. and Jin, W., 2021. Carbon Nanomaterials: Synthesis, Properties and Applications in Electrochemical Sensors and Energy Conversion Systems. *Materials Science and Engineering: B* 272. https://doi.org/10.1016/j.mseb.2021.115341.

Manawi, Y. M., Ihsanullah, Samara, A., Al-Ansari, T. and Atieh, M. A., 2018. A Review of Carbon Nanomaterials' Synthesis via the Chemical Vapor Deposition (CVD) Method. *Materials (Basel)* 11 (5). https://doi.org/10.3390/ma11050822.

Mohana, P., Isacfranklin, M., Yuvakkumar, R., Ravi, G., Kungumadevi, L., Arunmetha, S., Han, J. H. and Hong, S. I., 2024. Facile Synthesis of Ni-MgO/CNT Nanocomposite for Hydrogen Evolution Reaction. 14 (3), 280. https://doi.org/10.3390/nano14030280.

Muchlisha, N., Widjonarko, D. M. and Saraswati, T. E., 2023. Synthesis of Drug Carrier Carbon Nanofoam by Chemical Vapor Deposition Using Agar/NaCl Catalyst. *Journal of Physics: Conference Series* 2556 (1), 012006. https://doi.org/10.1088/1742-6596/2556/1/012006.

Nánai, L., Németh, Z., Kaptay, G. and Hernadi, K., 2024. Experimental and Theoretical Aspects of the Growth of Vertically Aligned CNTs by CCVD on Azo Substrate. *Scientific Reports* 14 (1), 7307. https://doi.org/10.1038/s41598-024-57862-w.

Prasiwi, O. D. I., Saraswati, T. E., Anwar, M. and Masykur, A., 2021. Magnetic Carbon Nanofibers Prepared with Ni and Ni/Graphitic Carbon Nanoparticle Catalysts for Glycine Detection Using Surface-Enhanced Raman Spectroscopy. *ACS Applied Nano Materials* 4 (7), 6594-6608. https://doi.org/10.1021/acsanm.1c00111.

Copyright © 2024, Universitas Sebelas Maret, ISSN 1412-4092, e ISSN 2443-4183

Priyanti, A. D. and Saraswati, T. E., 2021. The Differences of Physicochemical Characteristics of Graphene-Like Nanomaterials Directly Grown on Copper Foil and Quartz Substrate in Chemical Vapor Deposition (Cvd). *Journal of Physics: Conference Series* 1912 (1), 012028. https://doi.org/10.1088/1742-6596/1912/1/012028.

Saputri, D. D., Jan'ah, A. M. and Saraswati, T. E., 2020. Synthesis of Carbon Nanotubes (Cnt) by Chemical Vapor Deposition (Cvd) Using a Biogas-Based Carbon Precursor: A Review. *IOP Conference Series: Materials Science and Engineering* 959 (1), https://doi.org/10.1088/1757-899x/959/1/012019.

Saraswati, T. E., Prasiwi, O. D. I., Masykur, A. and Anwar, M., 2017. Bifunctional Catalyst of Graphite-Encapsulated Iron Compound Nanoparticle for Magnetic Carbon Nanotubes Growth by Chemical Vapor Deposition. *AIP Conference Proceedings* 1788 (1), https://doi.org/10.1063/1.4968282.

Saraswati, T. E., Priyanti, Ayu Dwi and Prasiwi, O. D. I., 2020a. Synthesis and Characterization of Carbonaceous-Based Nanomaterials Produced in Chemical Vapor Deposition (CVD) Using Copper Catalyst. *AIP Conference Proceedings* 2237 (1), https://doi.org/10.1063/5.0005445.

Saraswati, T. E., Priyanti, A. D. and Prasiwi, O. D. I. 2020b. Synthesis and Characterization of Carbonaceous-Based Nanomaterials Produced in Chemical Vapor Deposition (CVD) Using Copper Catalyst. *The 14th Joint Conference on Chemistry 2019*, https://doi.org/10.1063/5.0005445.

Speranza, G., 2021. Carbon Nanomaterials: Synthesis, Functionalization and Sensing Applications. *Nanomaterials (Basel)* 11 (4). https://doi.org/10.3390/nano11040967.

Wang, P., Song, Y., Mei, Q., Dong, W.-F. and Li, L., 2022. Sliver Nanoparticles@Carbon Dots for Synergistic Antibacterial Activity. *Applied Surface Science* 600. https://doi.org/10.1016/j.apsusc.2022.154125.

Zhang, D., Ye, K., Yao, Y., Liang, F., Qu, T., Ma, W., Yang, B., Dai, Y. and Watanabe, T., 2019. Controllable Synthesis of Carbon Nanomaterials by Direct Current Arc Discharge from the Inner Wall of the Chamber. *Carbon* 142, 278-284. https://doi.org/10.1016/j.carbon.2018.10.062.

Copyright © 2024, Universitas Sebelas Maret, ISSN 1412-4092, e ISSN 2443-4183